

51 MODES AND MECHANISMS OF DEGRADATION OF EPOXY-COATED REINFORCING STEEL IN A MARINE ENVIRONMENT

T. Nguyen and J.W. Martin

Building Materials Division, National Institute of Standards and
Technology, Gaithersburg, Maryland, USA

Abstract

Blasted-steel panels were coated with two commercial powder epoxy coatings at two thicknesses. Half of the coated panels were scribed; the other half remained free of defects. The panels were immersed in a saturated calcium hydroxide aqueous solution containing 3.5 % sodium chloride maintained at either 35 or 50 °C. Degradation was quantified by infrared thermography, wet adhesion test, and microscopic and analytical techniques. Unscribed panels exhibited only water-induced adhesion loss, but scribed specimens degraded by anodic blistering and cathodic disbondment, in addition to water-induced adhesion loss. Anodic blistering was attributed to localized crevice corrosion under coating followed by blistering via an osmotic pressure mechanism. Cathodic disbondment was caused by the alkalinity of the corrosion products at the cathodic sites. Water-induced adhesion loss was due to the presence of multiple layers of water at the coating/steel interface.

Keywords: Coating, concrete solution, corrosion, degradation, marine, rebars, steel,

1 Introduction

In 1974, the Federal Highway Administration (FHWA) sponsored a project at the National Bureau of Standards (now called the National Institute of Standards and Technology, NIST) to identify candidate organic coatings capable of protecting reinforcing steel bars from corrosion. Powder epoxy coatings emerged as the most promising of the coatings studied [1]. Since that time, over 100,000 structures containing powder epoxy-coated reinforcing steel bars (herein after called epoxy rebars) have been

Durability of Building Materials and Components 7 (Volume One). Edited by C. Sjöström. Published in 1996 by E & FN Spon, 2-6 Boundary Row, London SE1 8HN, UK. ISBN 0 419 20690 6.

constructed in the United States [2]. In general, the corrosion performance of structures containing epoxy rebars has been praiseworthy [3,4]. Recently, however, reports began to circulate about the premature deterioration of a number of substructural members in three bridges in Florida [5-7]. The negative impressions generated from these premature failures were reinforced by the poor condition of epoxy rebars in bridge decks located in several northern environments [8]. These findings led to declarations that 1) epoxy rebars are more susceptible to corrosion than bare steel rebars when exposed to a marine environment, 2) powder epoxy coatings are not effective in providing long-term corrosion protection to reinforcing steel in salt-contaminated concrete, and 3) the technology of epoxy-coated rebars, as practiced in North America, is flawed. Due to the seriousness of these findings, a study was initiated to reexamine the effectiveness of epoxy-coated rebar in a concrete substructural member exposed to a marine environment. This paper presents the modes and mechanisms of the degradation of powder epoxy-coated steel panels immersed in a saturated calcium hydroxide solution containing 3.5 % sodium chloride. Complete results of this study are presented elsewhere [9].

2 Materials and experimental procedures

Variables included in this study were: two commercial powder epoxy coatings, two coating thicknesses (130 and 190 μm), two coating conditions (unscribed and scribed), and two test temperatures (35 and 50 $^{\circ}\text{C}$). Two main experiments were conducted in parallel. The first experiment (corrosion test) followed the increase of the corroded area as a function of exposure time; while the second (wet adhesion test) tracked the loss in bond strength between the coating and steel substrate as a function of exposure time.

2.1 Materials

Four hundred (400) flat, hot-rolled steel panels from the same batch of steel and having dimensions of 152 x 102 x 3.2 mm were grit blasted to a white-metal finish, and had a roughness profile of 50-70 μm . After grit-blasting, each panel was individually wrapped in moisture resistant paper, which was not removed until the panel was coated. Two commercial, one-part powder epoxies commonly used for coating rebars were used; the glass transition temperatures of the two coatings were 85 and 115 $^{\circ}\text{C}$, as determined by differential scanning calorimetry.

2.2 Preparation of coated panels

The steel panels were randomly assigned to two groups; each group was coated with one epoxy coating. The coatings were applied to the substrate using a customized line of a rebar coating plant. In this process, the steel panels were heated to 214 $^{\circ}\text{C}$ for 11 minutes; electrostatically sprayed with the powder coating; and then cured at 204 $^{\circ}\text{C}$ for 11 minutes. The thickness of the coatings, which was controlled by the number of times the electrostatic gun passed over a panel, was measured at five locations on each panel using a thickness gauge. Only panels falling in the 92-152 ± 10 μm and 150-270 ± 25 μm thickness ranges were used. Coated panels were tested for holidays using a 67.5 V holiday detector; panels containing holidays were excluded from the study.

2.2 Preparation of specimens for exposure

Half of the panels in each group were incised with a 25.4 mm by 1 mm scribe mark, using a milling machine. For the corrosion test panels, the scribe mark was located in the center of the panel in a direction parallel to its longer side. For panels used in the wet adhesion test, the scribe was made at one end of the panel in the direction parallel to its shorter side. All scribe marks were visually inspected for cleanness and uniformity. A cylindrical ring of poly(methyl methacrylate) was bonded with a silicone adhesive to the top surface of each of the corrosion test panels. The silicone adhesive was allowed to cure for at least two weeks prior to filling the ring with the test solution. For wet adhesion test experiment, a rubber sealant was applied along the perimeter of each panel to contain the test solution. Detailed information on the specimen configurations for the corrosion and wet adhesion tests are given in References [9] and [10], respectively.

2.3 Exposure conditions

Coated panels were exposed to a test solution containing saturated calcium hydroxide, $\text{Ca}(\text{OH})_2$, and 3.5 % (by mass) sodium chloride, NaCl. (This solution resembles the pore solution in reinforced concrete used in a marine environment.) Half of the panels assigned to the corrosion experiment were immersed in the test solution heated at $35 \pm 1^\circ\text{C}$ and the other half were in the same solution at $50 \pm 1^\circ\text{C}$. The wet adhesion test was conducted at $35 \pm 1^\circ\text{C}$ only. In both experiments, the solution was continuously aerated by bubbling filtered and desiccated air through the solution. The oxygen concentration of the solution was periodically measured and found to be 7 ± 0.2 ppm (by volume). Test solutions were frequently replaced with fresh ones to ensure that the solution pH was maintained between 11.8 and 12.3.

3 Quantification of degradation

3.1 Infrared thermographic analysis

Blisters developed and grew near the scribe mark. The size and total area of these blisters were quantified using an infrared thermographic camera connected to a computer image analysis system described previously [11]. This technique has been demonstrated as a good, nondestructive way for quantifying the corrosion and blistering of coated metals. Figure 1 displays a typical thermographic image showing blisters along a scribe mark of a powder epoxy-coated panel exposed to the test solution.

3.2 Wet adhesion test

Cathodic disbondment and adhesion loss due to exposure were measured using a wet adhesion test apparatus described in Reference 10. The apparatus consisted of a 90° peel test fixture connected to a computerized universal testing machine. In this technique, the peel adhesion of the coating to the substrate was monitored while the coating was wet. All adhesion tests were conducted at room temperature and at a peel rate of 20 ± 0.1 mm per minute.

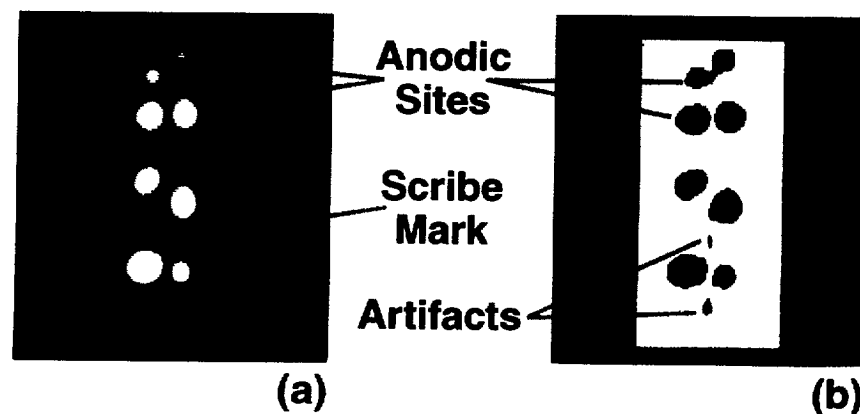


Figure 1. Thermographic image of the anodic blisters next to the scribe mark: a) thermographic image and b) computer enhanced image.

3.3 Microstructure and chemical analyses at degraded areas

3.3.1 Microstructural changes and distribution of chemical elements

After 500 h of immersion, several of the panels were removed from the exposure solution and 1 cm x 2 cm sections were cut perpendicular to the scribe length. These sections were prepared for microstructural and chemical analyses, using normal metallurgical procedures. The specimens were examined using a scanning electron microscope (SEM) equipped with a microprobe to determine the spatial distribution of Na^+ , Fe^{++} , Cl^- , and Ca^{++} ions through a cross-section of the scribe mark. In addition, pH of steel surface was measured after the wet adhesion test, using phenolphthalein indicator.

3.3.2 Concentrations of Na^+ and Cl^- ions and pH of fluid in the blisters

At the end of the immersion, several of the blisters were lanced with a hypodermic needle and the fluid removed. The pH and concentrations of Na^+ and Cl^- ions of the blister fluid were measured using pH, Na^+ and Cl^- selective microelectrodes.

4 Results

4.1 Degradation modes

Results from visual observations, adhesion tests, and chemical and microstructural analyses indicated that powder epoxy-coated steel panels containing no defects immersed in an aerated $\text{Ca}(\text{OH})_2$ solution containing 3.5% NaCl suffered only water-induced adhesion loss; the adhesion loss was mostly recovered upon drying. However, scribed panels exposed to the same conditions degraded in three modes: anodic

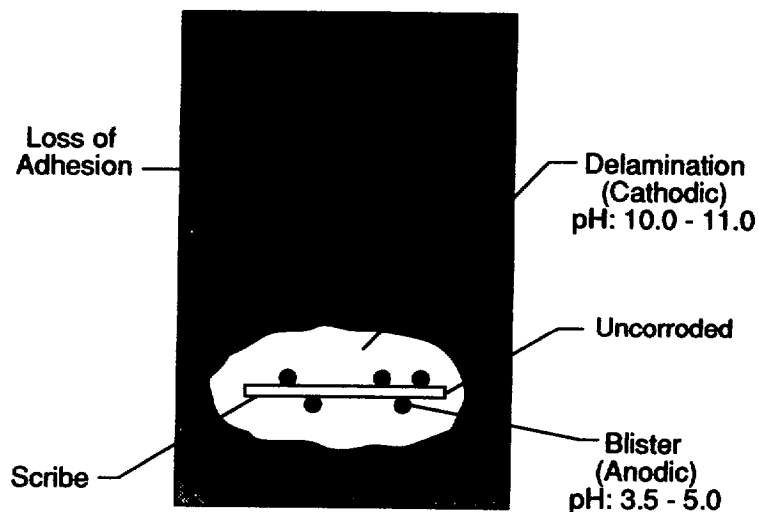


Figure 2. Three degradation modes of scribed epoxy-coated panels immersed in test solution.

blistering, cathodic disbondment, and water-induced adhesion loss. Figure 2 illustrates the three degradation modes and their relative locations on a scribed coated steel panel.

The characteristics of each degradation mode are described below.

4.1.1 Anodic blistering

The steel surface at the scribe mark remained uncorroded during exposure. However, anodes (i.e., corroded areas) were formed near and along the scribe mark within a few hours of immersion (see Figure 1). The total area covered by of the anodes increased with immersion time and the increase was faster at 50 °C than at 35 °C, as depicted in Figure 3. The growth of the anodic areas, $A(t)$, obeyed the power law model of the form:

$$A(t) = at^b, \text{ where } t \text{ is immersion time and } a \text{ and } b \text{ are constants.}$$

Multifactor analysis of variance study showed that the power law coefficients were not affected by coating thickness or coating type, but were significantly affected by the exposed temperature. That is, an increase of the exposure temperature decreased the induction time and increased the total anodic area.

After approximately 500h, blisters formed above each anodic area. The blisters contained pasty black corrosion products, mainly Fe_3O_4 . The steel substrate under the blisters was lost, as evidenced by both visual observation and SEM analysis. The solution in the blisters had a pH of between 3.5 and 5 and a Cl^- ion concentration 4-6 times greater than that of the bulk solution after 3000 h exposure. The concentration of Na^+ ion in the blisters was almost the same as that of the bulk. Elemental analysis also showed that the area under the blisters contained mostly Fe and Cl elements.

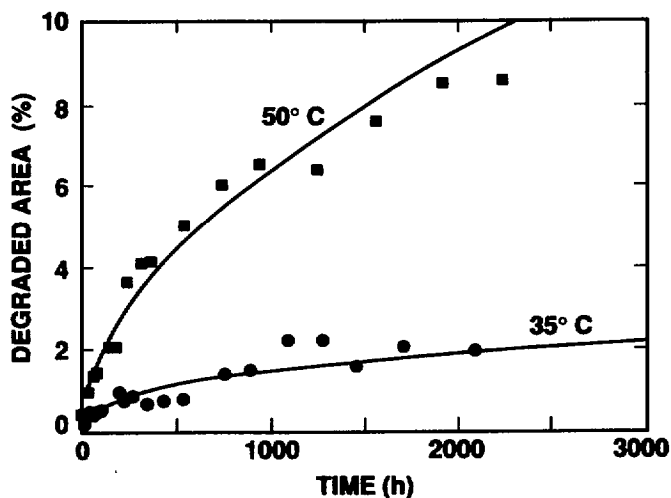


Figure 3. Growth of anodic blisters vs immersion time at 35 and 50 °C; symbols: experimental data; solid lines: power law model prediction.

These results indicated that the products formed inside the blisters was from the anodic half cell reactions of the corrosion process (hence the term anodic blisters).

4.1.2 Cathodic disbondment

The unblistered area in the vicinity of the scribe mark debonded from the steel substrate. After removing the coating, this area exposed a yellowish color and turned purple when treated with phenolphthalein indicator, suggesting that it had a pH of between 10 and 11. Based on these results, we postulate that the disbondment was due to the cathodic reactions (hence cathodic disbondment). The disbondment rate, which was independent of coating thickness or type, increased rapidly with immersion time up to 50 days but appeared to slowdown for longer exposure (Figure 4). This mode of failure was the most severe form of degradation of scribed epoxy-coated steel panels immersed in a saturated $\text{Ca}(\text{OH})_2$ solution containing 3.5 % NaCl.

4.1.3 Water-induced adhesion loss

The area beyond the cathodic disbondment lost some adhesion during exposure, which mostly regained upon drying (Figure 5). The steel surface in this area had a white-metal appearance. The demarcation between this adhesion loss and the cathodic disbondment zone can be easily observed by the naked eye and can be determined precisely by the wet adhesion test. The pH in this area was neutral, indicating the absence of $\text{Ca}(\text{OH})_2$ material. The loss of adhesion in this area was probably due to the presence of a layer of water at the coating/steel interface.

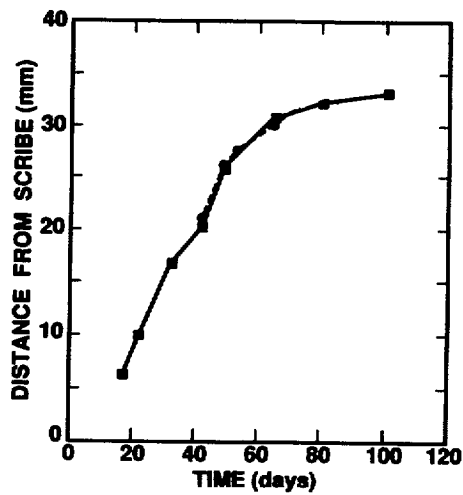


Figure 4. Cathodic disbonded distance from the scribe mark vs immersion time.

4.2 Mechanism

Figure 6 presents schematically the possible mechanisms of three degradation modes of a scribed epoxy-coated steel panel exposed to a saturated $\text{Ca}(\text{OH})_2$ solution containing 3.5% NaCl. The mechanisms of these modes are discussed below.

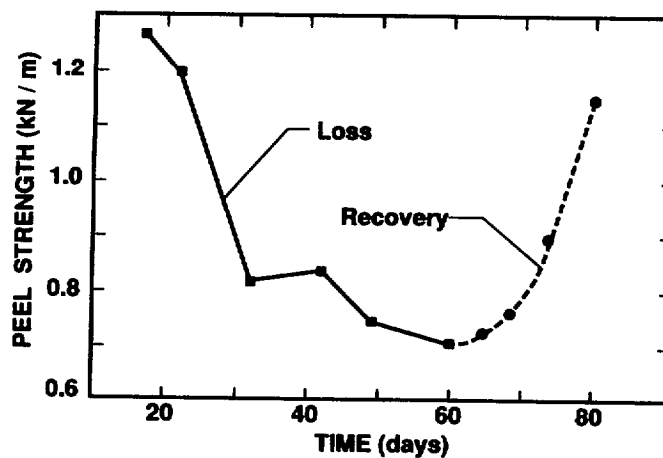


Figure 5. Water-induced adhesion loss and recovery as a function of immersion and drying time.

4.2.1 Anodic blistering

All microscopic and chemical analysis evidence obtained in this study showed that the blisters were formed at the locations where anodic (corrosion) reactions took place and that the characteristics of the products within the blisters were similar to those observed for crevice corrosion of bare steel, except that in this case the area of localized corrosion was between the coating and the steel substrate. Crevice corrosion apparently took place in areas along the scribe mark that were large enough to permit liquid entry but narrow enough to maintain a stagnant zone (12). For powder epoxy-coated steel immersed in saturated $\text{Ca}(\text{OH})_2$ containing NaCl , we believe that Cl^- ions migrated along the coating/steel interface from the scribe mark to a corrodable site underneath the coating where a corrosion cell was established. There were apparently two processes involving in the anodic blistering: anodic processes taking place at the "crevice" sites under coating followed by blistering at these sites.

The principal chemical processes taken place at the anodic sites under the coating in a chloride environment are reactions 1 to 3 given in Figure 6; these reactions are similar to those of localized corrosion of bare iron in a neutral chloride environment [13-15]. The main products at these locations are hydrated $\text{FeCl}_2 \cdot \text{H}_2\text{O}$ and Fe_3O_4 in equilibrium with saturated FeCl_2 [15]. Reactions 1 to 3 account for the presence of large quantity of chloride in the blisters, as observed in solution in the blisters as well as in the corrosion products on the steel surface after removing the coating [9]. The preferentially high concentration of Cl^- ions in the blisters is similar to that observed for localized corrosion of uncoated iron [12] and of organic coated steel in neutral chloride electrolytes [16]. In the absence of oxygen, the formation of Fe_3O_4 (Reaction 2 in Figure 6) is thermodynamically favored [15], consistent with our

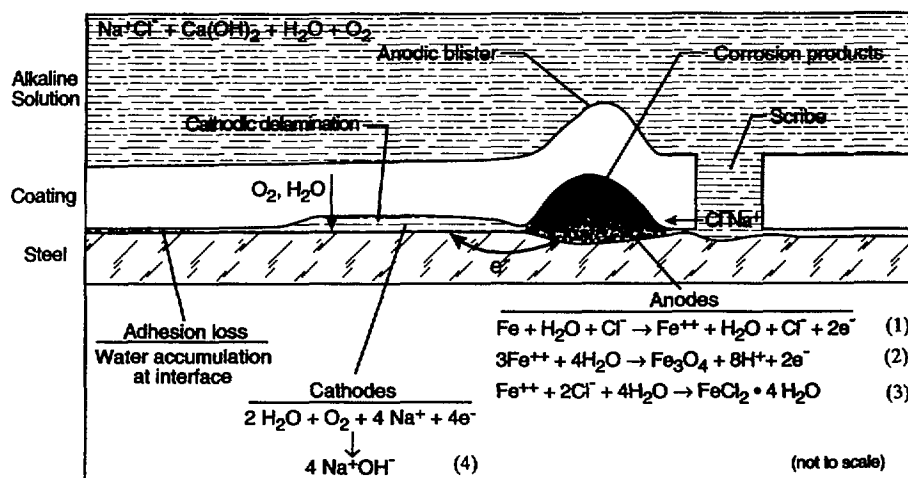


Figure 6. Proposed mechanisms of the degradation of scribed epoxy-coated steel panel immersed in a saturated $\text{Ca}(\text{OH})_2$ solution containing 3.5% NaCl .

observation of the black corrosion products in the blisters. The hydrolysis reactions (e.g., Reaction 2 in Figure 6) leads to the formation of HCl, which is particularly aggressive. This material accelerated the dissolution of Fe, which resulted in an increase of Cl⁻ ion migration to charge balance Fe⁺⁺ ions. The result was a rapidly accelerating, or autocatalytic, process at the bottom of the corroded sites under the coating.

The blistering process at the anodic sites was probably caused by an osmotic pressure mechanism. As hygroscopic products formed at the anodic sites, a thermodynamic water activity difference between these sites under the coating and the exposure environment was established. This set up an osmotic pressure gradient, which drove water from the outside to the anodic sites. Osmotic pressure has been proposed as the dominant mechanism responsible blistering of coatings systems exposed to neutral aqueous solutions (17). Electro-osmosis flow of water to the anodic regions, which accompanies Cl⁻ ions migration, and mechanical stress may contribute to the blistering process. Although the process of anodic blister formation may be understood, the exact location under the coating where corrosion cell was established is not known.

4.2.2 Cathodic disbondment

The main reaction at the cathodic sites is oxygen reduction (Reaction 4 in Figure 6) (13,18). In the presence of Na⁺ ions, the products at the cathodes were mostly NaOH (19,20). This reaction resulted in increased pH in the cathodic sites. In the initial stages, the separation between the anodic and cathodic sites may be negligible. However, as corrosion proceeded the transport of oxygen into the corroded sites can be limited because of the restricted convective flow of the liquid, the low solubility of oxygen in this electrolyte-concentrated liquid phase, and the low oxygen permeability of the corrosion products. Consequently, Reaction 4 ceased in this area because of lack of O₂. This resulted in a separation of the anodic and cathodic sites. However, the anodic reactions (Reactions 1-3) still continued on the steel surface because Cl⁻ ions can permeate through the anion-selective hydrated iron oxides and hydroxides to reach the steel surface.

As rust filled the corroded area, the cathodes moved to somewhere under the coating where O₂ and H₂O are abundant. At these locations, the bonding strength was completely lost with little recovery after drying [10]. We believe that loss of adhesion in this region was similar to that observed when a scribed, coated steel panel is exposed to a neutral chloride environment; this phenomenon has been studied extensively (18,20,21). Mathematical models for this degradation mode have been developed (20). The alkalinity of the products formed from the cathodic reactions (e.g., Reaction 4) is believed to be responsible for the disbondment. The pH at the delamination front as high as 14 has been reported for scribed panels exposed to a neutral chloride environment (22). The region of alkalinity associated with cathodic disbondment in this study could be seen clearly by the pH indicator and from the wet adhesion test results. Our diffusion experiment using atomic absorption spectroscopy showed no evidence of Na⁺ diffusion through the free films of the same coatings despite the fact these coatings contained numerous large pores. These results suggested that Na⁺ ions probably reached the cathodic sites by migrating along the coating/steel interface, consistent with other studies in neutral chloride environments (23,24).

4.2.3 Water-induced adhesion loss

The loss of adhesion, which largely recovered upon drying, in the region beyond the cathodic disbondment area (see Figure 2) was probably due to the presence of a water layer of many monolayers thick at the coating/steel (oxide) interface. (Steel surface is always covered with an iron oxide layer about 3-4 nanometers thick.) Adhesion loss in water or high relative humidities is commonly observed for polymeric coatings on a high energy substrate (25,26). The main reason for the presence of a water layer at the organic coating/iron oxide interface is that the weak secondary organic film/oxide bonds ($<25\text{kJ/mol}$) cannot resist the stronger affinity of water to the polar, high-energy iron oxide surface ($40\text{--}60\text{kJ/mol}$) (27,28). Thermodynamic analysis also revealed that polymer/oxide interfacial bonds are not stable in an aqueous medium and that water is capable of displacing the organic film from the substrate (26). This means that, if the steel surface is not modified, water is likely to enter coating/steel interface when a coated steel panel is exposed to an aqueous environment. Reference 25 gave numerous examples to support the presence of multilayers of water at the organic coating/metal interface. Further support comes from recent *in situ* study of water at the coating/substrate interface using sensitive spectroscopic technique (29).

5 Summary and conclusions

Four sets of epoxy-coated steel panels were prepared by applying two commercial epoxy powder coatings at two thicknesses. Scribed and unscribed epoxy-coated panels from each set were immersed in a saturated calcium hydroxide solution containing 3.5 % sodium chloride, at either 35 or 50 °C. The degradation was quantified by infrared thermography and wet adhesion techniques. The degraded areas were characterized by a number of microscopic and analytical techniques. Unscribed panels deteriorated only one mode: loss of adhesion due to a water layer at the coating/steel interface, which mostly regained after drying. However, scribed panels degraded in three different modes: anodic blistering, cathodic disbondment, and water-induced adhesion loss. Anodic blistering took place by two processes: crevice corrosion at the anodic sites followed by blistering at these sites via an osmotic pressure mechanism. Cathodic disbondment occurred away from the scribe and was caused by the alkalinity of the cathodic reaction products formed under the coatings. Water-induced adhesion loss, which was similar to that of the unscribed panels, took place beyond the cathodic disbondment region. A water film of many monolayers thick at the coating/steel interface was responsible for this adhesion loss.

6 Acknowledgements

The authors would like to thank Dr. Y. Paul Virmani of FHWA for his support and encouragement throughout this project and to FHWA for providing the research funds. The completion of this project was greatly facilitated through the help of Mr. Greg Weaver of Lane Enterprises, Inc., who coated the steel panels.

7 References

1. Clifton, J.R., Beeghly, H.F. and Mathey, R.G. (1974) Nonmetallic coatings for concrete reinforcing bars. *Federal Highway Administration Report No. FHWA-RD-74-18*.
2. Neff, T.L. (1992) Letter to specifiers of corrosion protection systems. *Concrete Reinforcing Steel Institute*, February.
3. Allen, J. (1993) Epoxy-coated rebar benefits Minnesota deck. *Roads and Bridges*, June, p. 38.
4. Burke, D.F. (1994) Performance of epoxy-coated rebar, galvanized rebar, and plain rebar with calcium nitrite in a marine environment. *Proceedings of the International Conference on Corrosion and Corrosion Protection of Steel in Concrete*, University of Sheffield, England, July.
5. Kessler, R.J., Powers, R.G. and Langley, R.M. (1986) Corrosion evaluation of substructure cracks in Long Key Bridge. *Florida Department of Transportation, Bureau of Materials and Research*, Corrosion Report No. 86-3.
6. Smith, L.L., Kessler, R.J. and Powers, R.G. (1993) Corrosion of epoxy-coated rebar in a marine environment. *Transportation Research Circular*, Vol. 403, p. 36.
7. Sagiés, A.A., Powers, R. and Kessler, R. (1994) Corrosion processes and field performance of epoxy-coated reinforcing steel in marine substructures. *Corrosion/94*, paper No. 299.
8. Clear, K.C. (1993) Effectiveness of epoxy-coated reinforcing steel (C-SHRP Report: Executive Summary, *Transportation Research Circular*, Vol. 403, p. 66.
9. Martin, J.M., et al. (1995) Degradation of powder epoxy-coated panels immersed in a saturated calcium hydroxide solution containing sodium chloride, *Report to the Federal Highway Administration*, July.
10. Alsheh, D., Nguyen, T. and Martin, J.W. (1994) Adhesion of fusion bonded epoxy coatings on steel in alkaline solution. *Proceedings of the Adhesion Society*, February, p. 209.
11. McKnight, M.E. and Martin, J.W. (1989) Detection and quantitative characterization of blistering and corrosion of coatings on steel using infrared thermography. *Journal of Coatings Technology*, Vol. 61, No. 775, p. 57.
12. Fontana, M.G. (1986) *Corrosion Engineering*, McGraw Hill, New York, 3rd ed., pp 51-59.
13. Cohen, M. (1979) Dissolution of iron, in *Corrosion Chemistry*, (eds. G.R. Brubaker and P.B.P. Phipps), *ACS Symposium Series 89*, American Chemical Society, Washington, D.C., pp 126-152.
14. McCafferty, E. (1981) Use of activity coefficients to calculate conditions within a localized corrosion cell on iron. *Journal Electrochemical Society: Science and Technology*, Vol. 128, p. 40.
15. Pourbaix, M. (1971) The electrochemical basis for localized corrosion, in *Localized Corrosion*, (eds. R.W. Staehle, B.F. Brown, J. Kruger, and A. Agrawal), National Ass. Corrosion Engineers, Houston, TX, pp 12-33.
16. Nguyen, T. and Lin, C. (1991) In situ measurement of chloride ion at the coating/metal interface. *Journal of Adhesion*, Vol. 33, p. 241.

17. Funke, W. (1981) Blistering of paint films and filiform corrosion. *Progress in Organic Coatings*, Vol. 9, p. 29.
18. Leidheiser, H. (1983) Towards a better understanding of corrosion beneath organic coatings, *Corrosion*, Vol. 39, p. 189.
19. Schwenk, W. (1981) Adhesion loss of organic coatings, causes and consequences for corrosion protection, in *Corrosion Control by Organic Coatings*, (ed. H. Leidheiser, Jr.), National Ass. of Corrosion Engineers, Houston, TX, p. 103.
20. Nguyen, T., Pommersheim, J. and Hubbard, J.B. (1995) A unified model for the degradation of organic coated steel in neutral electrolytes, *Journal of Coatings Technology*, in press.
21. Dickie R.A. and Smith, A.G. (1980) How paint arrests rust. *Chemtech*, Vol. 10, p.31.
22. Ritter, J.J. and Kruger, J. (1981) Studies of subcoating environment of coated iron using qualitative ellipsometric and electrochemical techniques, in *Corrosion Control by Organic Coatings*, (ed. Leidheiser, H., Jr.), National Ass. of Corrosion Engineers, Houston, TX, p. 28.
23. Stratmann, M., et al, (1994) The scanning Kelvinprobe -- a new technique for the in-situ analysis of the delamination of organic coatings, *Proceedings of the 20-th International Conference in Organic Coatings Science and Technology*, Athens, Greece, pp 519-531.
24. Funke, W. (1985) Toward a unified view of mechanism responsible for paint defects by metallic corrosion," *Ind. Eng. Chem. Prod. Res. Dev.*, Vol. 24, p. 343.
25. Leidheiser, H., Jr. and Funke, W. (1987) Water disbondment and wet adhesion of organic coatings on metals: a review and interpretation, *Journal of the Oil Colour Chemists Association*, Vol. 70, p 121.
26. Kinloch, A.J. (1983) *Durability of Structural Adhesives*, Applied Sci., N.Y., pp 1-38.
27. Bolger, J.C. and Michaels, A.S. (1969) Molecular structure and electrostatic interactions at polymer-solid interface, in *Interface Conversion for Polymeric Coatings*, Elsevier, N.Y, pp 3-60.
28. Thiel, P.A. and Madey, T.E. (1987) The interaction of water with solid surfaces: fundamental aspects. *Surface Sci. Rep*, Vol. 7, pp. 211-385.
29. Nguyen, T., Byrd, E. and Bentz, D. (1994) A study of water at the coating/substrate interface. *Journal of Coatings Technology*, Vol 66, No.834, p.39.